34th Annual International Conference of the IEEE EMBS
San Diego, California USA, 28 August - 1 September, 2012

Centerline calculation for extracting abdominal aorta in 3-D MRI images

Danilo Babin, Ewout Vansteenkiste, Aleksandra Pižurica and Wilfried Philips

Abstract— **The examination of abdominal aorta is an effective way to diagnose many cardiovascular diseases. Aortic stiffness measured by pulse wave velocity (PWV) calculation is a good estimate of overall cardiovascular health. Calculation of pulse wave velocity requires the length of abdominal aorta as an input parameter, while the structure of abdominal aorta can be used for diagnostic purposes. For the sake of non-invasive diagnostics, non-contrasted MRI images of aorta were used. Due to the "black-blood" imaging, a lot of artifacts are present and a robust centerline extraction method is needed. In this research we develop a novel graph-based method for extracting centerlines of abdominal aorta for length calculation. Our method is robust to artifacts and noise and applicable to any imaging modality.**

I. Introduction

Aortic stiffness is an important diagnostic factor that can be well estimated through the pulse wave velocity (PWV) measurement. For this, the length of the abdominal aorta between the points of interest needs to be calculated. The goal of this research is to extract the centerline of the abdominal aorta in 3-D MRI images. In order to achieve the non-invasive examination, the contrast fluid was not used in the scanning process, hence, the abdominal aorta appears as a black blood vessel (i.e. "black-blood" images). This poses a much harder segmentation problem due to the fact that the structures surrounding the aorta appear in the same range of (low) pixel intensities (lungs, veins and heart), where the tissues delineating these organs are often not well visible. This is clearly noticeable in the heart region, where the delineation between heart ventricles and aorta is not obvious. The non-contrasted images often contain artifacts due to heart movement and intense blood flow, causing the aorta not to be visible in some of the slices. Therefore, classical segmentation methods applied to this problem often produce inaccurate results containing regions of leakages.

The current reviews on vessel extraction techniques [1], [2] show a wide variety of methods developed for angiographic vessel images. However, the "black-blood" vessel extraction methods are rare. The methods working on "black-blood" vessel images are either not robust enough to deal with slice discontinuities and motion and flow artifacts [3] or are not fast enough [4]. Most common methods for segmentation of the abdominal aorta are the methods for segmenting aortic aneurysms, which work on angiographic images of much higher quality than in our case. The methods using deformable models [5] need fine parameter tuning to avoid leakages in MRI images, where different regions of the aorta might need to be segmented separately with different parameters. The existence of discontinuities of aortic regions in neighboring slices is also a problem which these methods are not able to cope with. The same problem arises for model based methods [6], where the multiple models for healthy and sick aortas might need to be specified separately. Methods based on the mathematical morphology [7], [8] are often used for vessel segmentation, but they are also no able to cope with the mentioned artifacts.

Our previous work on this problem was a segmentation algorithm described in [4], where we proposed a method that compares the pixel value to the average value of all pixels in the structuring element. The value assigned to the processed pixel is equal to the maximum size of the structuring element, thus prioritizing similar structures, and making the segmentation process less dependent on individual pixel values. In this paper we propose a method that extends this approach to centerline extraction. The main idea of our approach is to build a regular structured grid skeleton (considered as a graph), where the node and link values are sampled from the image using the described method [4]. The centerline of the aorta is extracted in a semi-automatic way, where the user has to specify the start and end point of a blood vessel. We design our algorithm to allow quick examination of multiple alternative paths for extraction of complicated vessel structures.

The paper is organized as follows. In Section II, we explain the proposed method. In four subsections we describe our previous work on the topic and its extension to centerline extraction for length measurement. In Section III, we present the results of our proposed algorithm and length measurement with the results of length measurements of hand-made expert centerlines. Section IV concludes this work.

II. The proposed method

We develop our method for vessel centerline extraction of non-contrasted MRI images, although the same method can be applied to centerline extraction of contrast-injected images. We base the proposed method on our previous work on *generalized profiles* (GP), described in [4], [9], which is a generalization of multi scale approach of morphological profiles [10].

All authors are with Department of Telecommunications and Information Processing-TELIN-IPI-IBBT, Faculty of Sciences, Ghent University, Sint-Pietersnieuwstraat 41, B-9000 Ghent, Belgium.
Danilo Babin: dbabin@telin.ugent.be
Ewout Vansteenkiste: ervsteen@telin.ugent.be
Aleksandra Pižurica: sanja@telin.ugent.be
Wilfried Philips: philips@telin.ugent.be

978-1-4577-1787-1/12/$26.00 ©2012 IEEE

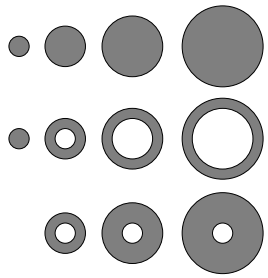

Fig. 1: An illustration of the proposed differential structuring element (DSE) compared to standard SE. Top row: SE with different size r, middle row: DSE with varying r parameter and constant n parameter, bottom row: DSE with varying n parameter and constant r parameter.

A. Generalized profiling

The basic idea of generalized profiling is to compare the pixel value to the characteristic value of all pixels in the (multi scale) structuring element, by which we determine the size of the neighborhood in which the current pixel is "darker" than its surrounding. One of the main novelties of GP method was the introduction of *differential structuring element* (DSE), defined as a subtract of two structuring elements $S(p)$ of different size:

$$D_{r,n}(p) = S_{r+n}(p) - S_r(p),\ r \in \{0, 1, ...\},\ n \in \mathbb{N}, \quad (1)$$

where r denotes the size of a smaller SE and parameter n is defined as the difference in sizes between the two SEs. This principle is illustrated in Fig. 1 in the case of spherical DSE. By definition, the SE of the size $r = 1$ is a window containing only the center pixel p, while the SE of the size $r = 0$ is an empty set. The advantage of this principle is that the DSE allows a wider range of neighborhood sets to be formed that in the case of SE. In general, the SE of any size can be expressed as a DSE with the r parameter set to zero ($r = 0$). Another novelty of GP method was the introduction of different functions applies to the whole set of values defined by the DSE:

$$f_D(r, n, p) = f(D_{r,n}(p)), \quad (2)$$

where f denotes a function applied to the DSE at pixel p for given parameters r and n. This value represents a given characteristic of the neighborhood $D_{r,n}$, depending on the particular choice of f. In this paper, we use only the average function ($f = avr$). For segmentation purposes, it is of interest to consider the 1-D vector obtained by varying the r parameter of the DSE, while keeping the n parameter to its lowest value ($n = 1$). This yields a vector of average functions applied to one pixel wide ring-shaped neighborhoods:

$$\mathcal{R}_{avr,D}(n = 1, p) = \{avr_D(r, n = 1, p),\ \forall r \in [0,\ r_{max}]\}. \quad (3)$$

Finally, the range in which the current pixel is darker than its surrounding d is calculated as the number of sequential components (starting from the first component) of vector $\mathcal{R}$, for which the all the vector components have a value higher than the value of the current pixel p:

$$d(p) = \max_{r_{max}}(avr_D(r, n = 1, p) > v(p),\ \forall r \in [0,\ r_{max}]). \quad (4)$$

Obviously, the "measure of darkness" is limited by the value r_{max}, which has to be chosen beforehand. In this paper we use the spherical (3-D) DSE with the maximum span of r_{max}=5 pixels.

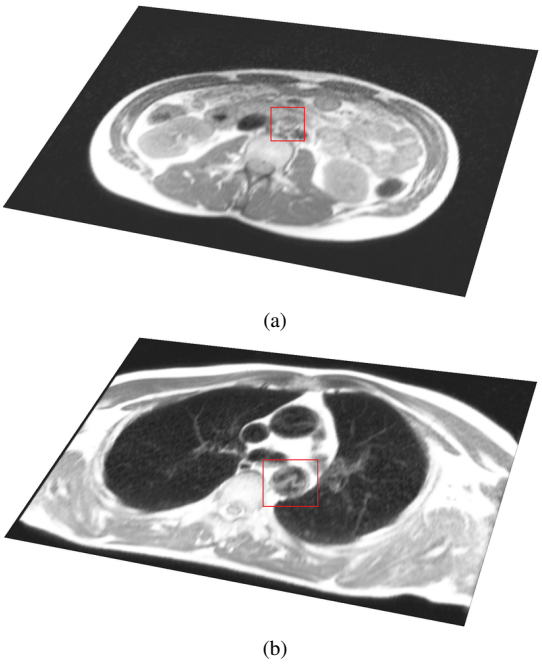

(a)

(b)

Fig. 2: Examples of artifacts found in "black-blood" MRI images marked in red: (a) aorta not visible in transversal slice, (b) noise in the aorta due to heart motion.

B. Data sets

The data sets we used consist of low quality (1.5T) non-contrasted MRI images, where a lot of noise and motion artifacts are present. The aim is to obtain valid results on structure of the aorta, while making the method non-invasive and as fast as possible. Hence, the 3-D data set was taken with a high inter-slice spacing of 6.6mm (pixel spacing is 1.32mm×1.32mm), which often causes the effect of single object not being connected in neighboring slices, making the segmentation of the given data set a hard task. Fig. 2 shows examples of artifacts found in the "black-blood" MRI data sets, where the aorta is often not clearly visible in a number of adjacent slices. For this reason, the centerline extraction method has to be robust, while requiring low amount of user interaction. The method should be general in order to allow the centerline extraction on other imaging modalities.

C. Creating the sampling grid

The centerline extraction method we propose in this paper is based on the careful construction of subsampling grid using our method of generalized profiling [9]. The main

advantage behind the subsampling in centerline calculation is to avoid artifacts that appear randomly in certain slices and to take into account only the subsampled positions which are "valid" positions inside the abdominal aorta. Another advantage of subsampling is that the calculation time is reduced when compared to the techniques that take every voxel of the 3-D image data set into account. We create an initial skeleton grid (graph) as a regular grid of arbitrary size. This means that the nodes of the initial grid are equally distributed with the constant spacing between them in all directions (x, y and z directions), which is determined by user specified number of sampling nodes in each of directions. Our experiments show that sampling grid of dimensions 20×20×20 results in the best balance of given results and needed execution times. It should be noted that specifying the region of interest for the algorithm can speed up the calculation and yield better end results.

Due to the regular spacing of nodes, some of the nodes of the regular grid get positioned in bright regions of the image which can not be the regions of the aorta. In order for all the nodes to be positioned in the dark regions of the image (which are candidates for the aortic regions), we propose to move the nodes to the darkest image region in the bounding area positioned between the nodes of the initial grid. This means that our algorithm searches for the darkest region around each node, where the search areas do no overlap. We define the position of the darkest region to be the pixel with the intensity belonging to the lowest 10% of searched values in the given node area, which has the highest profile value for average profile function, as defined in (4). When the center of the darkest region for a given node is located, the node of the grid is moved to the found position. In this fashion, we re-position the nodes in the darkest regions while making sure that the nodes will not overlap. Hence, the subsampling property of the grid is maintained. We finalize the grid construction by entering the values for the links connecting each node to its 6 closest neighbors from the initial grid. The metric value of a link m is calculated as the average of all the pixel intensities belonging to the straight line L connecting the two nodes of the link:

$$m_{link} = \frac{1}{n(L)} \sum_{i=1}^{n(L)} v(p_i), \tag{5}$$

where $v(p)$ represents the intensity of pixel p and $n(L)$ the number of pixels belonging to the line segment. Fig. 3a shows the modified grid of size 20×20×20, where the red color indicates higher link values and blue indicates lower link values.

D. Centerline extraction

In order for the centerline to be extracted, the user must specify the start and end position of the desired centerline path. These positions are entered into the existing sampling grid as new nodes, which we connect with their closest 6 nodes and enter the new link values as described by (5). Using the metrics stored in the links of the sampling grid,

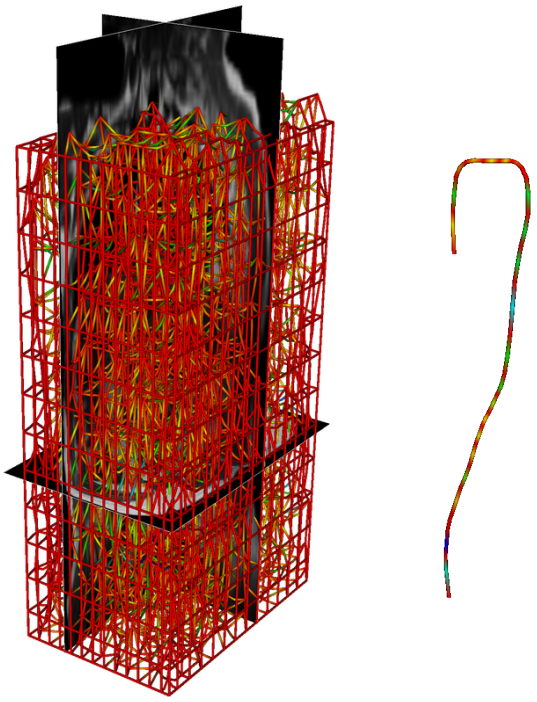

(a) (b)

Fig. 3: Illustration of sampling skeleton grid construction and centerline extraction. (a) shows the final sampling skeleton grid. The outer part of the grid is not modified due to the constant value of the background pixels. The nodes in the inner part of the grid converge to darker regions of the image. (b) extracted centerline of abdominal aorta after the graph converging and smoothing of the result.

the graph converges with respect to the entered start and end nodes separately. This means that the distances of all the nodes from the given start node are calculated, after which the distances of all the nodes from the given end node are calculated, using the Dijkstra's shortest path algorithm [11]. In this fashion, the final metric for each of the nodes m_{node} is calculated as the sum of distances from both the start and end node:

$$m_{node} = l(node, node_{start}) + l(node, node_{end}), \tag{6}$$

where $l(node1, node2)$ represents shortest path between $node1$ and $node2$ (obtained from the link metrics). We design our application to find the different paths between the desired nodes and to sort the obtained centerlines according to the calculated node metrics (in an ascending fashion). In order to take only different paths into account, the nodes belonging to a previously found centerline are not taken into account (since they will yield the same path that was already found). Finally, the obtained paths are smoothed by simple weighted averaging of neighboring positions in the calculated paths. The application is implemented in such a way that the user is able to scroll through the found and sorted centerlines and select the desired best path (centerline).

The advantage of our approach of converging graphs with respect to different nodes is that the extraction of complicated

TABLE I: Lengths of abdominal aorta obtained using our centerline extraction method and hand-made centerline extraction

Set	Our method (mm)	Ground truth lengths	Deviation (%)
1	363	374	2.94
2	407	415	1.92
3	399	396	0.75
4	386	376	2.59
5	387	395	2.02

paths can be performed using intermediate points, which are user specified. In that case the described algorithm is performed on a number of user specified nodes (in an ordered way), instead on only two points. In this fashion our proposed algorithm provides a way of interactive segmentation of images of a very low quality and high presence of artifacts. Moreover, our algorithm is applicable to different imaging modalities by changing the metrics used for graph converging (e.g. for contrast-enhanced images, the priority is given to the bright regions instead of dark ones).

III. Results

We tested our algorithm on five data sets of 3-D MRI images of "black-blood" abdominal aorta. The dimensions of the grid were $20\times20\times20$, and the maximal radius of spherical DSEs was set to 5 pixels. In each case the start and end node of the aorta were specified, and the resulting centerlines were obtained without needing to specify the intermediate centerline positions. The results depicted in Fig. 4 show that the extracted centerlines accurately represent the path and position of the abdominal aorta. The comparison of the lengths obtained using our centerline extraction method to lengths obtained by hand-made expert centerlines is given in Table I. The calculated lengths show that the absolute deviation falls under 3% in all five cases, which represents a highly accurate length calculation. The average execution time on a 2.4GHz processor is about 2 minutes.

The future work on this topic will consist of the implementation of centerline extraction based on a predefined model of the abdominal aorta, which will result in less user interaction.

IV. Conclusion

We introduced a novel centerline-extraction method and applied it to determining the path of abdominal aorta and calculating its length. The proposed algorithm uses advanced methods to create the sampling grid in order to deal with the intense artifacts found in the non-contrasted MRI images and to shorten the execution. Our method is semi-automatic, allowing arbitrary number of intermediate centerline points to be specified for extraction of complex paths. The advantage of our approach is that it is applicable to all imaging modalities, including the non-contrasted MRI images, allowing the non-invasive aorta examination. Obtained length calculation results show high accuracy when compared to results of expert hand-made centerlines.

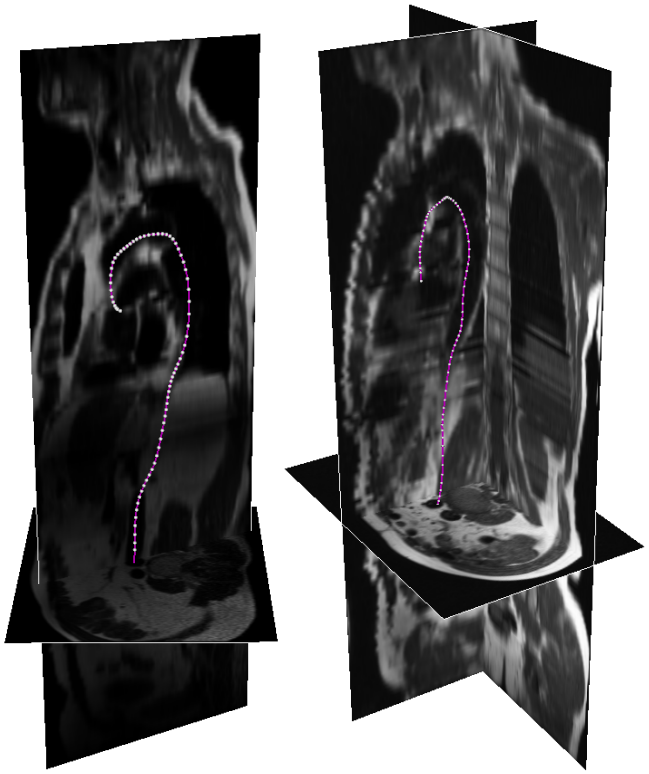

Fig. 4: Results of abdominal aorta centerline extraction accurately depict the path and length of the aorta.

References

[1] C. Kirbas, F.K.H. Quek: *A Review of Vessel Extraction Techniques and Algorithms*, ACM Computing Surveys 36 (2), p. 81-121, 2004.

[2] D. Lesage, E.D. Angelini, I. Bloch, G. Funka-Lea: *A review of 3D Vessel Lumen Segmentation Techniques: Models, Features and Extraction Schemes*, Medical Image Analysis, Elsevier, 2009.

[3] H. M. Ladak, J. B. Thomas, J. R. Mitchell, B. K. Rutt, D. A. Steinman: *A semi-automatic technique for measurement of arterial wall from black blood MRI*, Medical Physics, vol. 28, issue 6, 1098-1107, 2001.

[4] D. Babin, E. Vansteenkiste, A. Pižurica, W. Philips: *Segmentation and length measurement of the abdominal blood vessels in 3-D MRI images*, EMBC 2009 Proceedings:

[5] S. Loncaric, M. Subasic, E. Sorantin: *3-D deformable model for abdominal aortic aneurysm segmentation from CT images*, Proceedings of the First International Workshop on Image and Signal Processing and Analysis, 139-144, 2000.

[6] M. de Bruijne, B. van Ginneken, W. J. Niessen, M. Loog, M. A. Viergever:*Model-based segmentation of abdominal aortic aneurysms in CTA images*, Proceedings of Medical Imaging 2003: Image Processing, pp.1560-1571, 2003.

[7] J. Serra: *Image Analysis and Mathematical Morphology*, volume 1, Academic Press, 1982.

[8] P. Soille: *Introduction to Mathematical Morphology*, Comput. Vis., Graph., Image Process., vol. 35, pages 283-305, 1986.

[9] D. Babin, A. Pižurica, R. Bellens, J. De Bock, Y. Shang, B. Goossens, E. Vansteenkiste, W. Philips: *Generalized Pixel Profiling and Comparative Segmentation With Application to Arteriovenous Malformation Segmentation*, Medical Image Analysis, Elsevier, In press, 2012.

[10] M. Pesaresi, J.A. Benediktsson: *A New Approach for the Morphological Segmentation of High-Resolution Satellite Imagery*, IEEE Trans. Geosci. Remote Sens., vol.39, no. 2, Feb. 2001.

[11] E. W. Dijkstra: *A note on two problems in connection with graphs*. In Numerische Mathematik, 1, 269-271, 1959.